Surface Review and Letters, Vol. 5, Nos. 3 & 4 (1998) 769–781

STRAIN RELIEF VIA ISLAND RAMIFICATION IN SUBMONOLAYER HETEROEPITAXY

BERT MÜLLER,*†@ LORENZ P. NEDELMANN,* BJØRN FISCHER,* HARALD BRUNE,* JOHANNES V. BARTH,* KLAUS KERN,* DANIEL ERDÖS‡ and JOACHIM WOLLSCHLÄGER‡

*Institut de Physique Expérimentale, Ecole Polytechnique Fédérale de Lausanne, CH-1015 Lausanne, Switzerland

†Institut für Quantenelektronik, Eidgenössische Technische Hochschule Zürich, CH-8093 Zürich, Switzerland

‡Institut für Festkörperphysik, Universität Hannover, D-30167 Hannover, Germany

Received 19 May 1997

The mechanisms of strain relief in submonolayer heteroepitaxy of Cu/Ni(100) are studied using variable temperature scanning tunneling microscopy and high resolution low energy electron diffraction. It is demonstrated that pseudomorphic copper islands, as they grow in size, undergo a spontaneous shape transition. Below a critical island size of about 500 atoms the islands have a compact shape, while above this size they become ramified. The shape transition of the coherently strained islands, predicted theoretically by Tersoff and Tromp, is driven by the size-dependent outward relaxation of the step edge atoms due to the positive lattice mismatch. The ramified island shape, which reflects the energy minimum of binding and strain energy, is characterized by only one parameter: the arm width of the monolayer-high copper islands $w = (22 \pm 1)$ atoms.

1. Introduction

Thin film structures with smooth interfaces are critically important for studying the effects of reduced dimensionality in electronics, optics and magnetism. To produce thin epitaxial layers, rather sophisticated growth techniques such as molecular beam epitaxy (MBE) are required since most of the applications need highly pure materials with a minimum of morphological and structural defects. MBE is essentially a nonequilibrium phenomenon governed by the competition between growth kinetics and thermodynamics. Control and manipulation of MBE growth requires a detailed understanding of this competition. At low substrate temperatures/high deposition rates the dominance of kinetics can be used to tailor artificial structures.[1]

In heteroepitaxial growth, in addition to the kinetic constraints, the strain energy due to the misfit between substrate and adlayer has to be considered. The minimization of the associated strain energy can result in defect structures of the adlayer which are very stable and might even appear at submonolayer coverages. For instance, we have recently demonstrated by scanning tunneling microscopy (STM) that the compressive strain of submonolayer copper films on Ni(100) is relieved via lateral relaxation of atoms from hollow to bridge sites.[2,3]

Surface-sensitive methods are essential for understanding the phenomena in epitaxial growth and the underlying physics. STM is especially well suited for studying the elementary growth processes on an atomic scale. In particular, through the availability of variable temperature STM, the very early stages of epitaxial growth can be quantitatively studied by analyzing the island density, island size distribution and island shape as a function of substrate

@Present address: Eidgenössische Materialprüfungs- und Forschungsanstalt CH-8600 Dübendorf, Switzerland

temperature.[4–7] Thus it was, for example, possible to verify the validity of nucleation theory on an atomic scale[5] and to understand and simulate the fractal and dendritic growth on hexagonal close-packed surfaces.[8–13] Such growth has not been observed on square surfaces, since the barrier for edge diffusion is substantially higher on triangular than on square lattices due to the presence of twofold-coordinated edge sites in the close-packed directions. On square lattices, the barrier for edge diffusion is usually even lower than for terrace diffusion and the fabrication of dendritic and fractal islands is inhibited. Hence, lattices with a square symmetry are particularly suitable for the study of strain effects on island shapes.

Strained epitaxial islands are expected to be unstable against shape changes.[14–16] Analyzing the relation between strain energy and island shape in heteroepitaxial growth, Tersoff and Tromp[17] have predicted a spontaneous shape transition during the growth of the coherently strained islands. Shape changes were predicted to be a major mechanism of strain relief. But, up to now, experimental evidence for strain-induced shape transitions has been rather scarce. It is related to the growth of three-dimensional, flat pyramids with a rectangular basis.[17–19] Here, we present the first experimental verification of such a shape transition in the growth of monolayer-high islands. For the experiments, we have chosen a simple metal-on-metal system, Cu/Ni(100). The two metals are chemically very similar, their lattice mismatch is quite small (2.6% compressive strain), and they do not show any reconstruction. Submonolayer growth experiments performed between 250 and 370 K reveal that small islands exhibit the expected compact shape, whereas larger islands (exceeding a critical size of ≈ 480 atoms) become ramified. This island-size-dependent shape transition is quantitatively treated in the present paper.

2. Experimental

The growth of copper islands on Ni(100) at submonolayer coverages has been studied by variable temperature STM *in situ* but *after deposition*; the analogous experimental setup has been described elsewhere.[20] The Ni(100) crystal was prepared by cycles of argon ion sputtering (1 μA/cm^2) at room temperature as well as at elevated temperatures (about 550 K) and subsequent annealing (up to 1400 K) resulting in dislocation-free terraces up to a width of a few thousand angstroms. Copper was deposited by thermal evaporation from a Knudsen type MBE source at background pressures in the 10^{-10} mbar range. The deposition rate was varied between 6×10^{-5} and 3×10^{-2} ML/s and calibrated from STM images at monolayer coverage. The sample was heated by electron bombardment from the back side, whereby the substrate temperature (250–1400 K) was determined by a Ni/CrNi thermocouple fixed at the sample. The thermocouple was calibrated using liquid nitrogen, dry ice (solid CO_2), and a water/ice mixture before and after a series of experiments. The STM measurements were performed in the constant current mode at 0.5–2.0 V positive or negative bias and 0.5–8.0 nA tunneling current.

For the quantitative analysis of the island shapes we have only used images, where the thermal drift was negligible. Drift correction was therefore not necessary. The influence of structural defects such as substrate steps has been excluded by depicting areas far away from such defects. We can definitely rule out the possibility that the observed shape transition is due to coalescence, but there may be a very few of the large islands, especially those grown at low substrate temperatures (high island densities), which may be affected by coalescence.

The high resolution low energy electron diffraction (SPA-LEED) experiments were performed in a different ultrahigh vacuum chamber[21] using the same preparation procedures. For the intensity oscillation measurements, the external gun was used operating at an energy of 90 eV. Here, the deposition rate was calibrated from the intensity oscillations due to the layer-by-layer growth at low substrate temperatures as well as from the quartz microbalance.

3. Characterization of the Island Shape Transition

Copper forms two-dimensional islands of monolayer height on Ni(100).[22] Examples of monatomic-high islands which clearly show an irregular shape are shown in Fig. 1. As already pointed out in the introduction, it is surprising to find ramified islands on a square lattice. Edge diffusion at surfaces with square symmetry was reported to be comparable to terrace diffusion,[23–25] and therefore compact islands are generally expected. It is thus reasonable to assume

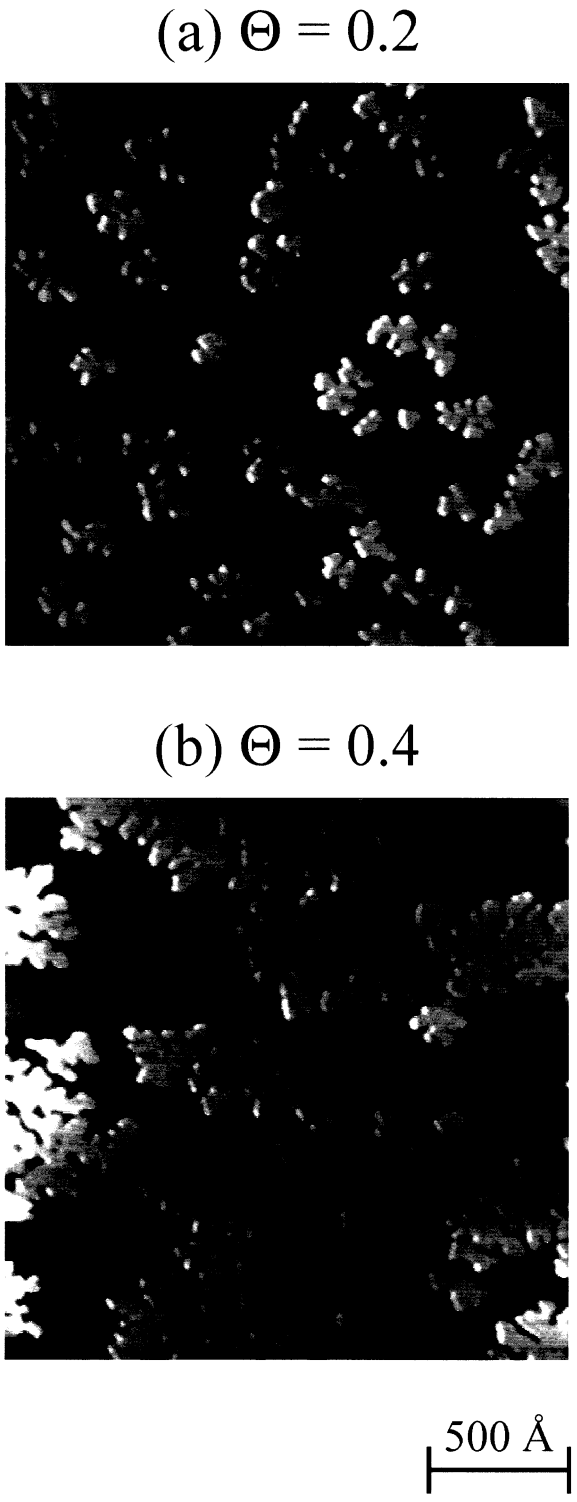

Fig. 1. Ramified island growth in submonolayer heteroepitaxy for Cu/Ni(100). The substrate temperature of 350 K and the deposition rate of 1.5×10^{-4} ML/s indicate that the islands are in equilibrium and their ramified shape is due to strain relief.

that the ramified copper islands on Ni(100) are not of kinetic origin. In order to confirm this assumption, we have systematically varied the substrate temperature and the deposition rate. A qualitative comparison for different growth conditions is given in Figs. 2 and 3. The images on the left hand side are obtained at high substrate temperature/low growth rate and exhibit, therefore, a low island density, whereby the images on the right which are obtained at low temperature/high growth rate show a higher island density. The island shapes, however, depend only on the average island size and are not affected by the growth conditions. Small islands always have a compact shape. As they grow in size, their shape becomes irregular. Almost all islands larger than the critical island size of about 500 atoms are ramified and the very large islands even exhibit a preferential arm width of about 20 atoms. The step edges of the island are preferentially oriented parallel and perpendicular to the substrate steps in the close-packed $\langle 110 \rangle$ directions. At substrate temperatures between 250 and 370 K the adsorbed copper atoms are very mobile on terraces and at step edges.[22] This temperature range even includes a transition in critical nucleus from $i = 1$ to $i = 3$[22] associated with dimer bond breaking. Therefore, the growth kinetics do not determine the island shape, and we can conclude that the island shapes correspond to an equilibrium configuration.

Analogous behavior (temperature and flux invariance) has been observed for another mechanism of strain relief of Cu/Ni(100), i.e. the internal {111} faceting.[2,3] This strain relief mechanism is already operative at submonolayer coverages and starts as soon as the compact part of the islands reaches a critical size of 1200 atoms. Monatomic chains of copper atoms are shifted laterally from the fourfold-coordinated hollow site to the twofold-coordinated bridge site and thereby protrude from the surface layer (see Fig. 4). For multilayer films, with each copper layer added, the protrusion stripes grow in width by one atom, forming internal {111} facets. These stripes disappear only if the sample is annealed above 550 K. We have observed both a reduction in stripe width as well as a reduction in stripe density, before they finally disappear, indicating the onset of alloying. Alloy formation has a dramatic effect not only on the internal faceting but also on the island

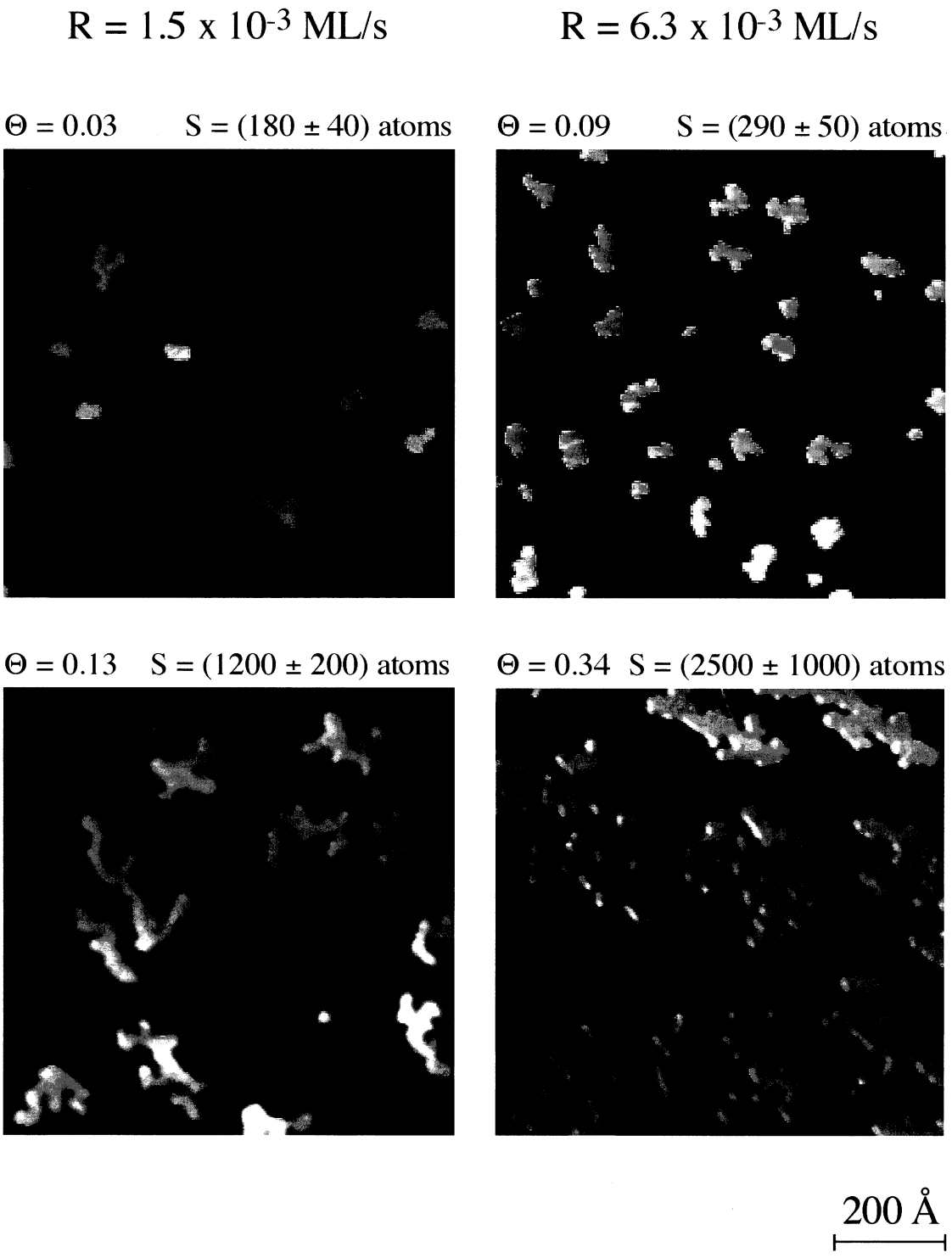

Fig. 2. The transition from compact to ramified island shapes at two different deposition rates (1.5 and 6.0 × 10^{-3} ML/s) and a fixed substrate temperature of 345 K. The coverages and the mean island sizes are indicated.

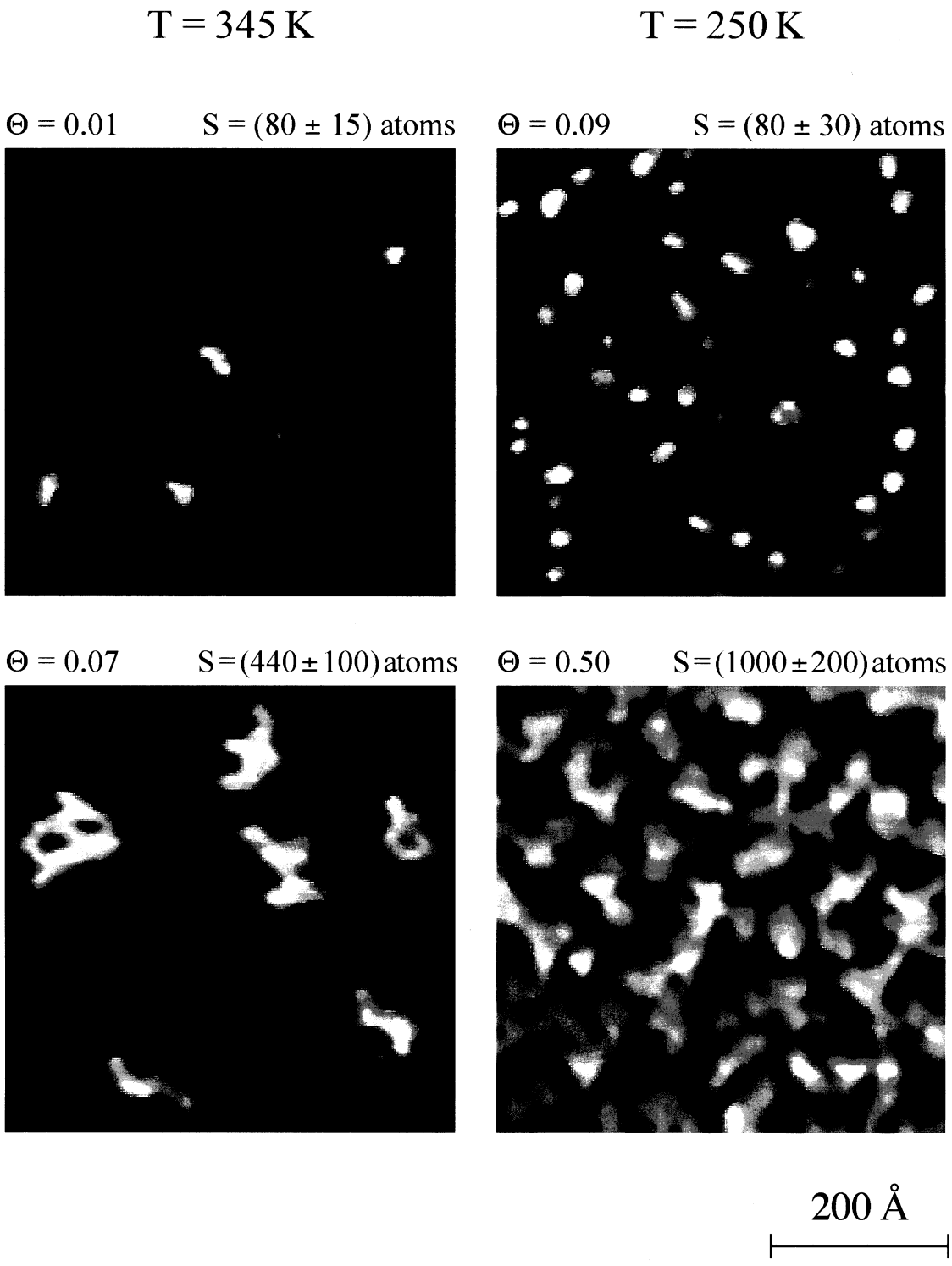

Fig. 3. The transition from compact to ramified island shapes at two different substrate temperatures (250 and 345 K) and a fixed deposition rate (1.5×10^{-3} ML/s). The coverages and the mean island sizes are indicated.

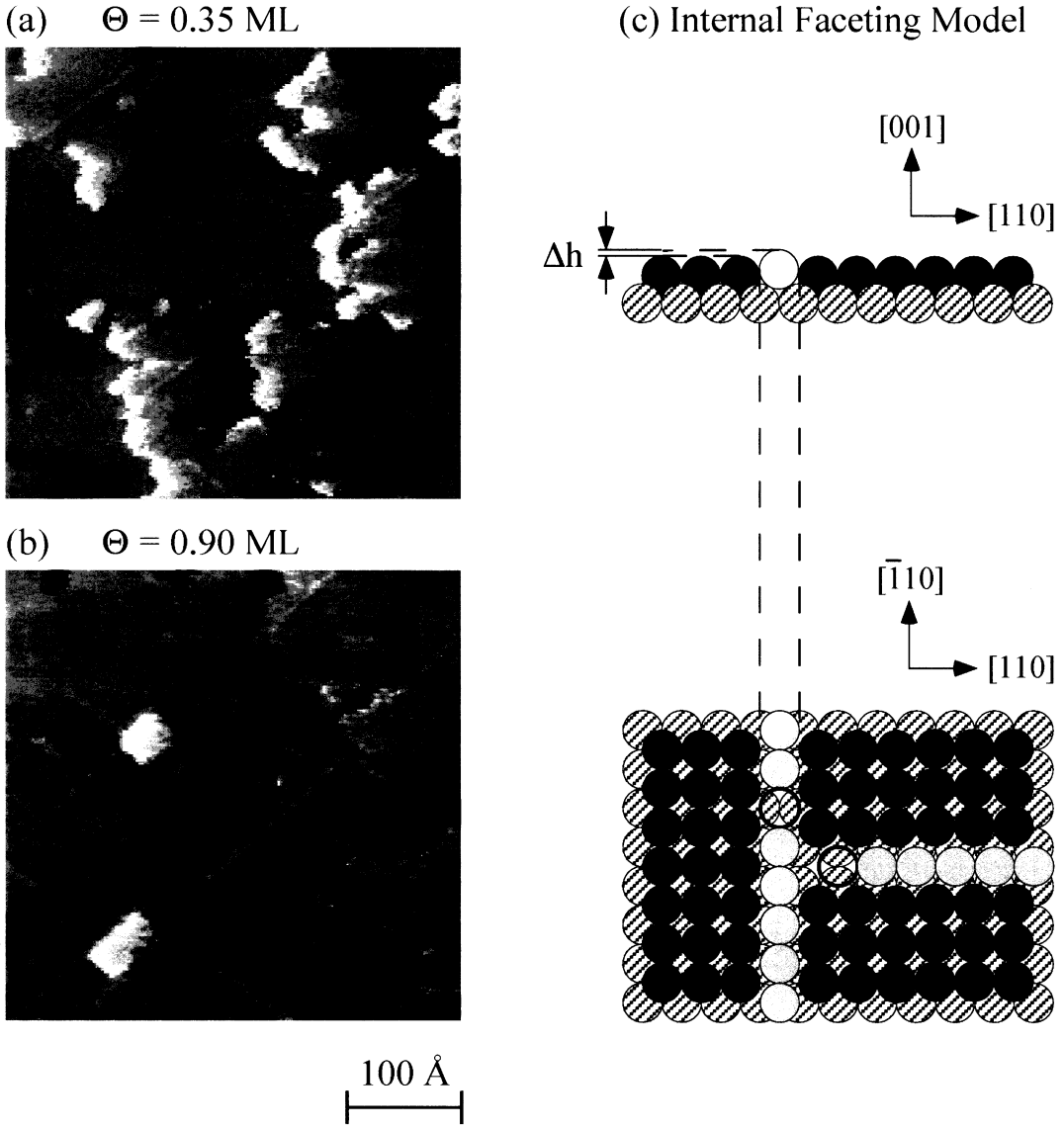

Fig. 4. Dislocations form at copper islands on Ni(100) at higher coverages to relief compressive strain.

ramification. After deposition below the critical temperature for surface alloy formation ($T < 400$ K) we annealed the sample to 500 K. The images presented in Fig. 5 demonstrate that upon intermixing of copper and nickel, compact islands form again. For this experiment, a temperature was chosen where the islands are not yet dissolved but exchange processes between Cu islands and the Ni substrate already occur. The effect of intermixing can be most easily seen at the step edges, which are straightened and become spotted. The rims are not well separated from the Ni substrate step and a rather irregular interface is formed. The islands are imaged with the same height and exhibit a similar spotted surface, and hence consist also of randomly mixed nickel and copper. Since the incorporated Ni atoms are smaller, the strain energy of the islands is significantly reduced[26] and consequently compact islands form.

4. Quantitative Analysis of the Island Shape Transition

The independence of the island shape from the growth conditions is confirmed by the quantitative

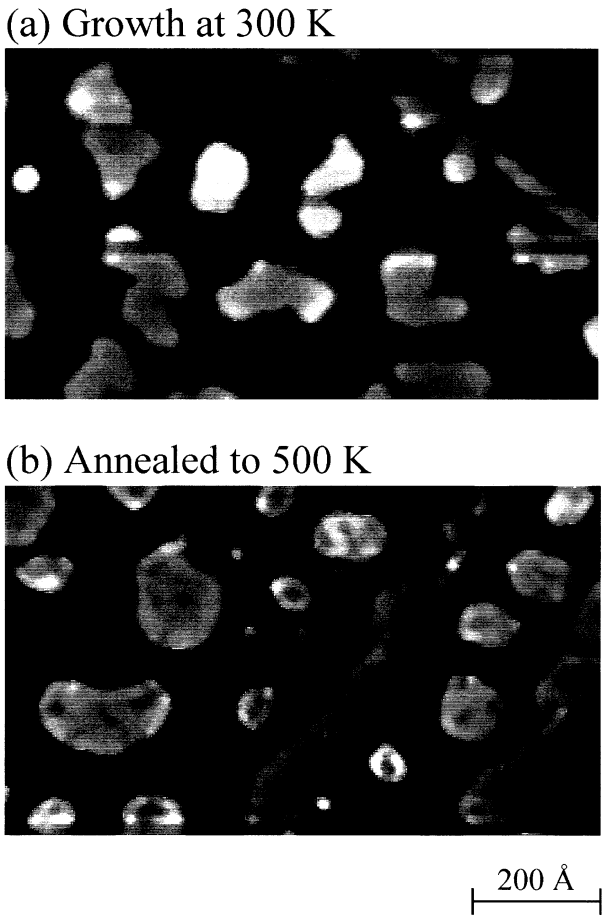

Fig. 5. STM images of islands and step edges for a 0.3 ML copper film on Ni(100) before and after annealing to 500 K, demonstrating the effect of surface alloying on the islands and at the step edges. The substrate temperature during growth was 300 K and the deposition rate 1.5×10^{-3} ML/s.

analysis of the topography of more than 3000 islands grown at very different substrate temperatures (250–370 K) and deposition rates ($6 \times 10^{-5} - 3 \times 10^{-2}$ ML/s). Indeed, all data collapse into one curve if one determines, for example, the island radius of gyration vs. island size (Fig. 6) or the island perimeter vs. island size (Fig. 7). The evaluation of the radius of gyration vs. island size, varied over four orders of magnitude, reveals a fractal dimension close to 2 ($D = 1.9$). This rather compact structure of the islands can be qualitatively recognized in the images of Fig. 1 — even for very large islands, the arms are separated only by narrow channels. This substantiates the previous statement that the island

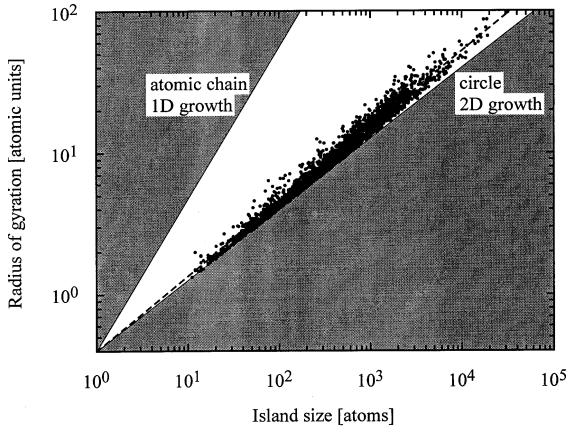

Fig. 6. Double-logarithmic plot of the islands' radius of gyration versus island size, demonstrating the coincidence of data obtained at different growth conditions. Each dot represents one island. The forbidden regions are gray in color; the upper limit is given by a one-atom-wide chain; the lower limit is an island of circular shape.

ramification cannot be understood in terms of a fractal growth mode of kinetic origin.

The evaluation of the island perimeter (p) as a function of island island size (A) is more helpful for gaining insight into the physics behind the island shape transition. It is displayed as a double-logarithmic plot in Fig. 7. Islands which contain less than 300 atoms exhibit always a compact shape. Their perimeter scales with the square root of the island size. For larger islands a deviation from this behavior is observed, and the dependence cannot be described in simple analytical terms, until for island sizes exceeding $\approx$ 3000 atoms the island perimeter is found to be directly proportional to the island size. This behavior can be modeled by the growth of a linear chain with a certain arm width w. Using this model, the arm width is obtained fitting the data for the islands which exceed the critical island size to $p = 2A/w + 2w$. Since $p(A)$ is given by the the experimental data, the arm width w is the only fit parameter. Several fits for island sizes above the critical value were performed and give almost identical results. Using the data of the island sizes above 1000 atoms, one obtains $w = (21.98 \pm 0.25)$ atoms, whereas for island sizes above 400 atoms, $w = (21.87 \pm 0.18)$ atoms. The arm width $w = 22 \pm 1$ is thus almost independent of the starting point. The critical island size, extracted with the linear chain model, is therefore $A_c = w^2 = (480 \pm 20)$ atoms.

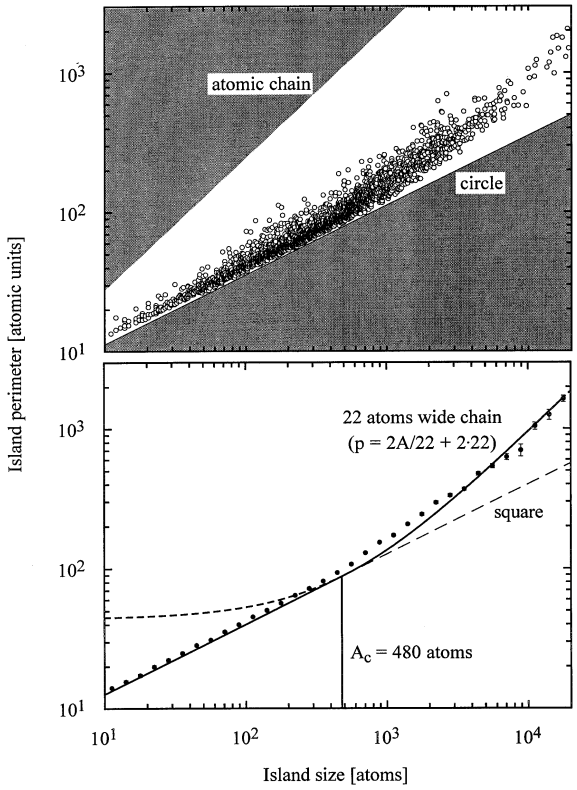

Fig. 7. (a) Island perimeter p vs. island size A for submonolayer copper islands on Ni(100) obtained for the same data as those presented in Fig. 6. The gray shaded areas are the forbidden regions for the ratios; the upper limit corresponds to that of circular islands and the lower limit to that of a one-atom-wide chain. (b) Averaged data displayed with statistical error bars. The data are compared with the linear chain model, where $p = 2A/22 + 2 \cdot 22$ (solid line).

5. Thermodynamics of Coherently Strained Islands

Tersoff and Tromp[17] have derived an expression for the energy of coherently strained (i.e. dislocation-free) epitaxial islands. They have considered three-dimensional, pyramid-shaped islands of width s, length t and height h on a square substrate. Minimizing the total energy, including the excess surface and strain energy, they have found a spontaneous shape transition with increasing island size. Small islands have a compact, symmetric shape while above a critical island size they become elongated, which allows better strain relaxation. While only the simple rectangular shape was studied, the basic result should be equally applicable to the ramified shape of the monolayer-high islands, particularly if the arm length substantially exceeds its width. With respect to a rectangular island width s, the branching of the ramified islands with arm width w does not affect the perimeter for a given island size.

The model of Tersoff and Tromp[17] is based on different assumptions:

(1) Corner effects are neglected. (Kink sites are energetically unfavored and occur, therefore, infrequently.)
(2) The surface energies of the substrate and of the islands are assumed to be equal.
(3) The strain does not change perpendicularly to substrate surface.

These assumptions are not severe limitations for the application to the present system:

(1) We have found a preferential orientation of the island step edges in the close-packed directions, and consequently corner effects are small.
(2) The surface energies of substrate and adlayer are comparable.[27]
(3) Perpendicular strain cannot change for monatomic-high islands. Hence, the approximate formula derived from Tersoff and Tromp should describe the system Cu/Ni(100). Cu/Ni(100) is a suitable candidate for checking the predictions of this theory in a quantitative manner.

In the model, the excess surface and strain energy is given by [Eq. (5) in Ref. 17]

$$E = b(s+t) - s\ln(t) - t\ln(s)\,. \qquad (1)$$

Here, E is the normalized energy accounting for the extra surface energy and the energy change due to elastic relaxation, b is supposed to be a constant consisting of elastic constants, and s and t are the island width and length, respectively. Since the island size $A = st$, one finds that

$$E = b\left(s + \frac{A}{s}\right) - s\ln\left(\frac{A}{s}\right) - \left(\frac{A}{s}\right)\ln(s)\,. \qquad (2)$$

Minimizing E with respect to s, one obtains two identical solutions up to the critical island size $A_c = \exp(2b+4)$ and two different solutions for the islands larger than A_c. Above A_c the width s shrinks from $s_c = \exp(b+2)$ to $s_\infty = \exp(b+1)$. This behavior is shown in Fig. 8. Because we cannot directly measure the width s and the length t due to the ramified

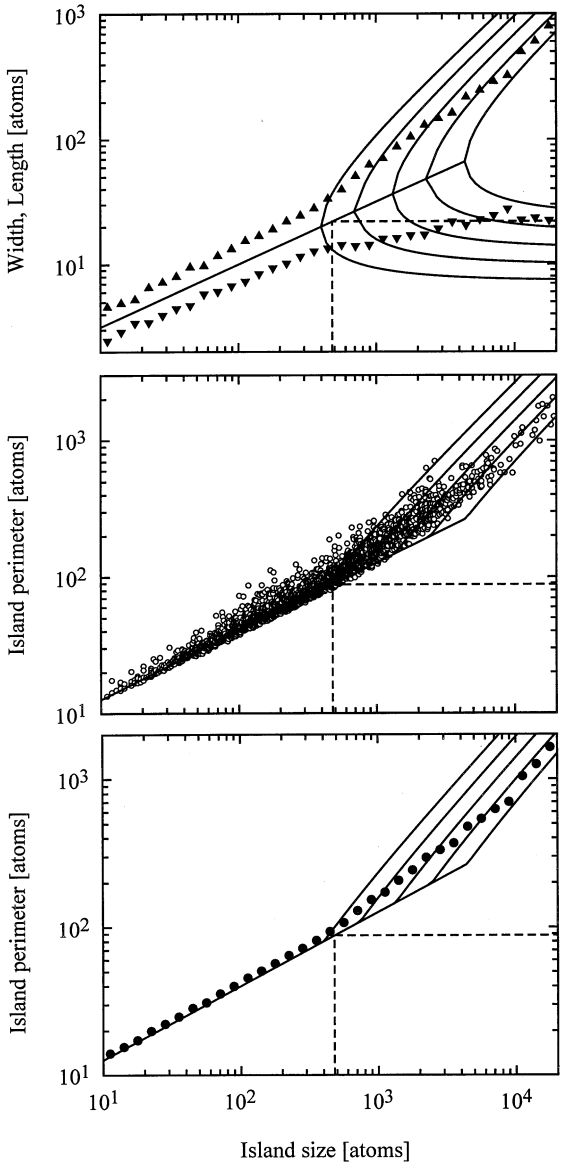

Fig. 8. Comparison between the model of Tersoff and Tromp[17] with $b = 1.0$, 1.3, 1.6, 1.9, 2.2 and the experimental data. An increase of b shifts the shape transition to higher island sizes. In Fig. (a) width s and length t are derived from perimeter p and island size A assuming a rectangular island shape and compared with the prediction from the model. Figures (b) and (c) contain the data shown in Fig. 6.

morphology of the islands and the existence of two equivalent close-packed directions, we have derived both values from the island perimeter and island size assuming a rectangular island shape. Up to the critical island size both s and t grow with the square root of the island size, as expected for compact islands. Above A_c they show the predicted splitting, whereas the width does not shrink but reaches a constant value. This discrepancy between model and experimental data is due to the particular, ramified shape of the two-dimensional islands. The model, a quasi-one-dimensional description, does not account for the growth in two equivalent directions and for finite size effects at the ends of the arms. Although the shrinking of the arm width is not present in the data of Fig. 8, it is clearly visible in Figs. 1(a) and 1(b). The island in the upper left of Fig. 1(a), for example, shows a clover-leaf-like structure, since only the inner part of the island develops the shrunk arm width. The larger islands [cf. Fig. 1(b)] are, therefore, also almost compact, only narrow channels are formed, and the arms (distance between neighboring channels) are thinner at the center of the island than in the outer part. This outer part, however, dominates $p(A)$ even for our largest islands, so that shrinking is not observable in the data of Fig. 8. Hence, from the physical point of view, the transition for Cu/Ni(100) should be described by $b = 1.1$ although higher values, e.g. 2.0, fit better the data. A value of $b = 1.1$ leads to $A_c = 500$ atoms, $s_c = 22$ atoms, and $s_\infty = 8$ atoms. These quantities are clearly obvious in the STM images: 500 atoms is, indeed, the critical island size, 22 atoms the critical arm width and the arms at the center of an island exhibit a width of approximately 8 atoms. (The reason that we do not find this behavior at each island in a similar manner is the weak driving force for diffusion due to the flat energy minimum.)

The width s in Eq. (2) can be replaced by the perimeter, and then one obtains the dependence between p and A within this model. This result is compared with the experimental data in Fig. 8. It is obviously impossible to find a specific value of b which describes the whole curve due to the discussed finite size effects in the marginal zones of the islands. Even if we take into consideration very large islands of 10^4 atoms, the rim of about 22 atoms dominates $p(A)$. Therefore, we have detected for such large islands an arm width of 22 atoms corresponding to the critical arm width and not the asymptotic arm width of 8 atoms. This is understood as the reason for the continued transition between two-dimensional and one-dimensional growth whereas the model predicts a sharp transition at A_c. The equilibrium theory in

the present status does not include these important effects and, therefore, fails in the quantitative description of our data. Nevertheless, the theory correctly predicts the spontaneous shape transition between two-dimensional and one-dimensional growth of monolayer-high copper islands on Ni(100) due to lattice strain, and our experiments are the first direct verification of the theoretical predictions of Tersoff and Tromp.

6. Relaxation of Edge Atoms at the Island Perimeter

The driving force for the observed preferential arm width and thus for the ramification of the copper islands on Ni(100) is associated with the positive lattice mismatch of the two materials. The effect of compressive strain forces the copper atoms to shift outwards from the island's center. The behavior is especially important for the step edges, since the step edge atoms are bound only to one side and are, therefore, free to relax outwards. They follow their natural lattice spacing, which is larger than that of the substrate material. On the other hand, the lower coordination of the edge atoms favors (size-dependent) inward relaxation[28] since less coordination tends to shrink bond length. In general, these two effects compete and it is *a priori* difficult to determine the dominant term. For the particular case of Cu/Ni(100) we have performed calculations using effective medium theory (EMT)[24] which reveal indeed a significant outward relaxation of the edge atoms, confirming the dominance of strain effects. The result for a relative small rectangular island is shown by a hard sphere model in Fig. 9.

The observation that the ramification of the islands involves preferential growth along the closed-packed directions, indicates that there is high mobility along the edges and that kink sites are energetically unfavorable. Both indications are corroborated by the EMT results. As for other square lattices, the barrier for edge diffusion (285 meV) is found to be lower than for terrace diffusion (469 meV) and the barrier for corner diffusion (530 meV) is only slightly larger. Kink sites are energetically costly since they reduce coordination while leaving the number of edge atoms constant. Corner sites, however, are not very stable because these atoms are relaxed outwards with respect to both closed-packed directions, giving rise to rounded corners. The formation of a constant arm width also implies that the island growth becomes anisotropic and atoms attaching sideways diffuse towards a tip.

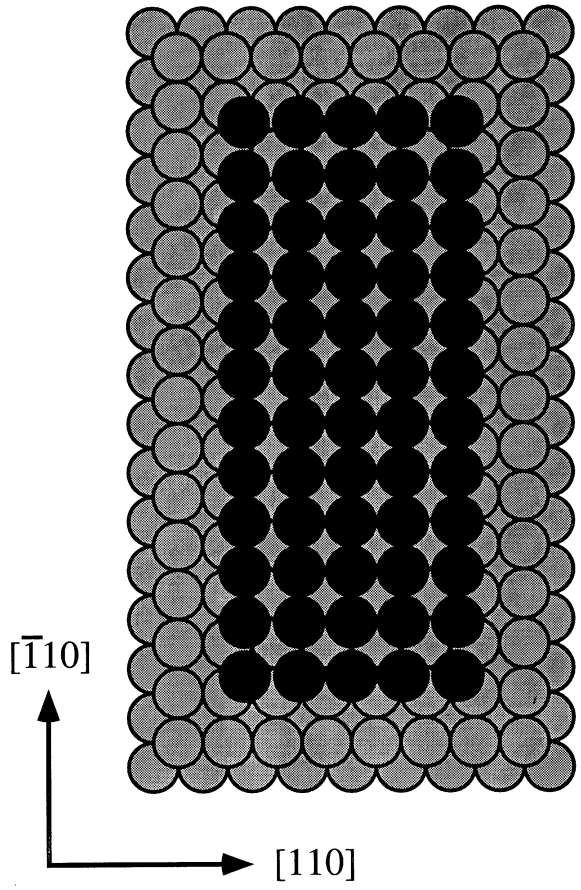

Fig. 9. Hard sphere model of a copper island on Ni(100) illustrating, with an exaggeration by a factor of 30, edge atom relaxation of compressively strained heteroepitaxial islands. The values for the outward relaxation are obtained from effective medium theory calculations.

Experimental evidence for the relaxation of step edge atoms of monatomic-high copper islands on Ni(100) is provided by high resolution low energy electron diffraction (SPA-LEED) data. The intensity of the specular beam has been recorded at different substrate temperatures and at a scattering condition close to out-of-phase where the electrons scattered at adjacent terraces interfere destructively so that the experiment has maximum sensitivity for monatomic steps.

During the initial growth at high substrate temperatures (350 K), we have found the well-known behavior that the intensity decreases immediately after

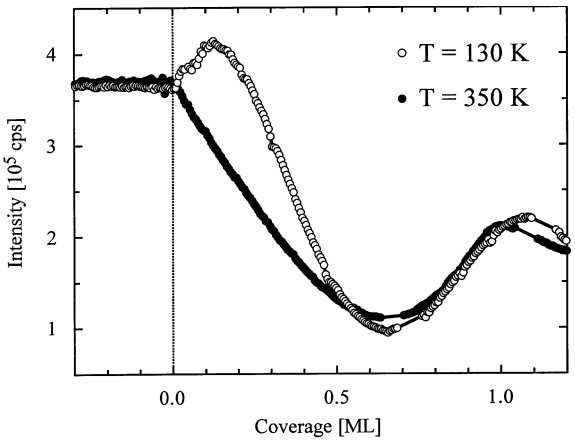

Fig. 10. Peak intensity of the specular beam during the initial stages of epitaxial growth of Cu/Ni(100), illustrating the different scattering behavior of step edge and terrace atoms.

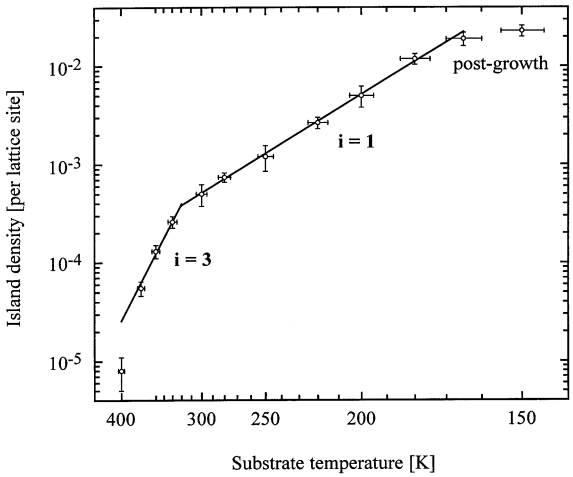

Fig. 11. Arrhenius plot of the measured saturation island density of Cu on Ni(100) (flux 1.5×10^{-3} ML/s; coverage 0.1 ML).

opening the shutter due to the formation of islands leading to an increasing destructive interference of the specular beam (cf. Fig. 10). At low substrate temperature, e.g. 130 K (cf. Fig. 10), we observe a considerable intensity overshoot which has to be expained. Up to now such phenomena have been attributed to the smoothening of the substrate by the diffusing adatoms which nucleate at residual defects. Here, however, the temperature behavior contradicts this explanation since we observe the increasing intensity for low substrate temperature. Therefore, we conclude that this phenomenon is due to a difference in scattering behavior between the copper atoms at step edges (or in small islands) and on terraces. The island density differs for the two substrate temperatures by two orders of magnitude (see Fig. 11). That means that the only difference for the two growth conditions during the very early stages of growth is the relative number of step edge atoms, which is much larger at the low growth temperature. Hence, for the present system the step edge atoms must have an enhanced reflectivity with respect to the terrace atoms. (The quantitative considerations will be a topic of a forthcoming publication.[29]) Besides this effect one observes that the intensity minimum is not exactly located at a coverage of 0.5 ML but significantly shifted to higher values. It has been demonstrated in previous papers[30,31] that this shift can be caused by the different scattering amplitude of (terrace) substrate atoms and (terrace) island adatoms neglecting form factor effects of the step edge atoms. For Cu/Ni(100), however, we have already shown in a previous study,[32] depositing multilayer films at high substrate temperatures in step flow mode, that the difference in scattering amplitude is small. Hence, the shift of the intensity minimum can only be explained by a significant amount of step edge atoms at half-monolayer coverage showing a higher reflectivity. For coverages between 0.7 and 1 ML, the density of edge atoms is not very different for the different growth temperatures due to coalescence (in the low temperature regime) and ramified island growth (in the high temperature regime), consistent with the occurrence of the well-pronounced minimum. At monolayer coverage, however, the island density is again higher for the low temperature regime and, therefore, we find a shift of the maximum to a coverage higher than 1 ML.

The intensity oscillations during the submonolayer growth of copper on Ni(100) can only be explained by a different scattering behavior of copper atoms at terraces and step edges which may be caused by the outward displacement of the step edge atoms from the ideal hollow site.

The two strain relief mechanisms — island ramification and stripe formation — have in common the fact that they involve displacements of atoms from the ideal pseudomorphic hollow site. For very small islands the strain can be relieved at the step edges

even if they have a compact shape. Larger islands become ramified to optimize the ratio between perimeter and island size. Finally, the stripes appear when the strain relief at the island edges is no longer sufficient for minimizing the total energy of the coherently strained islands. While the critical arm width is 22 atoms in the case of ramification, the typical island width for the onset of stripe formation corresponds to about 40 atoms.

The conclusion that ramification of islands is caused by the outward edge relaxation of copper atoms on Ni(100) due to the compressive strain is supported by the fact that copper forms ramified islands on Ni(100) but not on Pd(100),[33] although the two substrate materials are very similar. The copper islands are compressively strained on Ni(100) and exhibit tensile strain on Pd(100) due to the positive and negative misfit, respectively.

7. Determination of Strain Energy from Island Shape

The equilibrium island shape is understood as a result of the energy balance of the atomic bond energy within the islands and the strained energy due to the lattice mismatch with the substrate. Therefore, one can estimate the strain energy by the determination of the bond energy difference between the observed ramified islands and square islands of identical size. On the other hand, the islands try to attain compact shapes to optimize their binding energy. On the other hand, the strain energy associated with the island relaxation favors ramification. Based on bond counting, atoms inside of an island have four nearest neighbors in the adlayer, i.e. they are associated with two bonds per atom, whereas edge atoms have only three nearest neighbors in the adlayer associated with 1.5 bonds per atom. Therefore, the binding energy of an island corresponds to $(2A - p/2)E_b$, where A and p are expressed in the number of atoms forming the island and its perimeter, respectively. The binding energy per atom is therefore $(2 - p/2A)E_b$. For a square island, $p = 4\sqrt{A}$, and the bond energy per atom is given by $(2 - 2/\sqrt{A})E_b$. For the ramified islands, however, we have found that $p = 2A/22 + 2 \cdot 22$, which results in a bond energy per atom of $(2 - 1/22 - 22/A)E_b$. Hence, in this simple bond counting model, for very large islands, this energy gain of forming square-shaped with respect to ramified islands, E^* is 1/22 of the dimer bond energy E_b per atom.

The dimer bond energy can be derived from the Arrhenius behavior of the island density in the saturation regime, when the size of the critical nucleus is larger than 1 and the migration barrier is known.[4] [The case of Cu/Ni(100) is discussed in Ref. 22, in detail.] In general, the value E_b is associated with a very large error bar, since there are usually only a few data in a rather narrow temperature interval (cf. Fig. 11). For the present study, we have assumed that the attempt frequency for the $i = 1$ and for the $i = 3$ regime is identical, in agreement with our previous study and other authors'. A combined fit using all data of the $i = 1$ and $i = 3$ regimes including their error bars results not only in a well-determined value for the migration barrier but also for the dimer bond energy. The obtained values for the migration barrier (0.37 ± 0.03) eV, for the attempt frequency $5 \times 10^{(11 \pm 1)}$ Hz, and for $E_b = (0.34 \pm 0.03)$ eV confirm our previous study, but the error bar of E_b is reduced by a factor of 6 since the intersections of the $i = 1$ and $i = 3$ curves with ordinate are well defined due to the combined fit. E_b corresponds exactly to the value predicted by Evans and Bartelt[34] for a transition temperature of 320 K based on kinetic Monte Carlo simulations.

Using $E_b = (0.34 \pm 0.03)$ eV, the energy gain E^* corresponds to (15 ± 2) meV per island atom. This value, which is comparable to strain energies calculated from bulk properties, is relatively small and it is reasonale to assume that the difference can be overbalanced by the energy gain associated with the more effective strain relief at the longer edges of ramified islands. On the other hand, it is high enough to explain that the arm width is constant over the wide temperature range of 250–370 K.

8. Conclusion

The strain relaxation at the edges of copper islands on Ni(100) drives a transition from compact to ramified islands at a critical island size of about 500 atoms. The ramified islands exhibit a preferential arm width of (22 ± 1) atoms, which is associated with anisotropic strain relief. The phenomenon, predicted theoretically by Tersoff and Tromp, is expected to be of great importance in heteroepitaxy on square lattices with a positive lattice misfit. The present

experiments show that ramified island shapes cannot only be caused by growth kinetics at low temperatures but also by strain relief at rather high temperatures.

MBE growth, which is a dynamic, nonequilibrium phenomenon, is characterized by the competition between growth kinetics and thermodynamics. While thermodynamics embodies the essence of the behavior of the adlayer/substrate system at an equilibrium, kinetics controls the pathway of the system towards an equilibrium state within the thermodynamic limitations. These limitations reduce drastically the variety of nanostructures which can be tailored by the choice of the growth conditions. The present study gives an example of thermodynamic limitations: the ramified island growth at submonolayer coverages due to the lattice strain in heteroepitaxy cannot be outwitted by the choice of substrate temperature and deposition rate. On the other hand, one can employ this phenomenon to realize particular nanostructures even at rather high substrate temperatures. These nanostructures, which represent an equilibrium state of the heterosystem, should be quite stable because they are formed within a very large range of growth conditions.

Acknowledgments

Financial support from the Alexander von Humboldt-Stiftung (B. M.) and the Deutscher Akademischer Austauschdienst (L. N.) is gratefully acknowledged. We are grateful to Karsten Bromann (EPFL), Jerry Tersoff (IBM, Yorktown Heights) and Ivan Biaggio (ETHZ) for valuable discussions.

References

1. H. Röder, E. Hahn, H. Brune, J. P. Bucher and K. Kern, *Nature* **366**, 141 (1993).
2. B. Müller, B. Fischer, L. Nedelmann, A. Fricke and K. Kern, *Phys. Rev. Lett.* **76**, 2358 (1996).
3. B. Müller, L. Nedelmann, B. Fischer, A. Fricke and K. Kern, *J. Vac. Sci. Technol.* **A14**, 1878 (1996).
4. J. A. Venables, G. D. T. Spiller and M. Hanbücken, *Rep. Prog. Phys.* **47**, 399 (1984).
5. H. Brune, H. Röder, C. Boragno and K. Kern, *Phys. Rev. Lett.* **73**, 1955 (1994).
6. M. C. Bartelt and J. W. Evans, *Phys. Rev.* **B46**, 12675 (1992).
7. J. G. Amar and F. Family, *Phys. Rev. Lett.* **74**, 2066 (1995).
8. R. Hwang, J. Schröder, C. Günther and R. J. Behm, *Phys. Rev. Lett.* **67**, 3297 (1991).
9. H. Brune, C. Romainczyk, H. Röder and K. Kern, *Nature* **369**, 469 (1994).
10. H. Röder, K. Bromann, H. Brune, and K. Kern, *Phys. Rev. Lett.* **74**, 3217 (1995).
11. M. Hohage, M. Bott, M. Morgenstern, Z. Zhang, T. Michely and G. Comsa, *Phys. Rev. Lett.* **76**, 2366 (1996).
12. H. Brune, K. Bromann, J. Jacobsen, K. Jacobsen, P. Stoltze, J. Nørskov and K. Kern, *Surf. Sci. Lett.* **349**, L115 (1996).
13. Z. Zhang, X. Chen and M. G. Lagally, *Phys. Rev. Lett.* **73**, 1829 (1994).
14. M. A. Grinfeld, *Sov. Phys. Dokl.* **31**, 831 (1986).
15. D. Srolovitz, *Acta Metall.* **37**, 621 (1989).
16. B. J. Spencer, P. W. Voorhees and S. H. Davis, *Phys. Rev. Lett.* **67**, 3696 (1991).
17. J. Tersoff and R. M. Tromp, *Phys. Rev. Lett.* **70**, 2782 (1996).
18. Y.-W. Mo, D. E. Savage, B. S. Swartzentruber and M. G. Lagally, *Phys. Rev. Lett.* **65**, 1020 (1990).
19. T. Kuhlmann, B. Müller and K. Lischka, in preparation (1997).
20. H. Brune, H. Röder, K. Bromann and K. Kern, *Thin Solid Films* **264**, 230 (1995).
21. U. Scheithauer, G. Meyer and M. Henzler, *Surf. Sci.* **178**, 441 (1986).
22. B. Müller, B. Fischer, L. Nedelmann, H. Brune and K. Kern, *Phys. Rev.* **B54**, 17858 (1996).
23. C.-L. Liu, *Surf. Sci.* **316**, 294 (1994).
24. P. Stoltze, *J. Phys. Condens. Matter* **6**, 9495 (1994).
25. P. Ruggerone, C. Ratsch and M. Scheffler, in *Growth and Properties of Ultrathin Epitaxial Layers,* eds. D. A. King and D. P. Woodruff (Elsevier, Amsterdam, 1997), in press.
26. J. Tersoff, *Phys. Rev. Lett.* **74**, 434 (1994).
27. R. Kern, G. Le Lay and J. J. Metois, in *Current Topics in Material Science,* ed. E. Kaldis (Elsevier, Amsterdam, 1979), p. 131.
28. J. Fassbender, U. May, B. Schirmer, R. M. Jungblut, B. Hillebrands and G. Güntherodt, *Phys. Rev. Lett.* **75**, 4476 (1995).
29. B. Müller, J. Wollschläger and K. Kern, to be published (1997).
30. M. Henzler, in *Kinetics of Ordering and Growth at Surfaces,* ed. M. G. Lagally (NATO ASI, New York, 1990), p. 101.
31. J. Wollschläger and A. Meier, *Apl. Surf. Sci.* **104/105**, 392 (1996).
32. L. Nedelmann, B. Müller, B. Fischer, K. Kern, D. Erdös and J. Wollschläger, *Surf. Sci.* **376**, 113 (1997).
33. E. Hahn, E. Kampshoff, N. Wälchli and K. Kern, *Phys. Rev. Lett.* **74**, 1803 (1995).
34. M. C. Bartelt, L. S. Perkins and J. W. Evans, *Surf. Sci.* **344**, L1193 (1995).